energy&fuels

pubs.acs.org/EF

Article

# Combined Influence of High Pressure and High Temperature on the Removal of Crude Oil from Water during Laboratory-Scale Gas Flotation

Martina Piccioli, Robert André Gjelsten Larsen, Marcin Dudek, Svein Viggo Aanesen, and Gisle Øye*

Cite This: *Energy Fuels* 2023, 37, 5644−5651

Read Online

ACCESS | Metrics & More | Article Recommendations | Supporting Information

**ABSTRACT:** Produced water (PW) is the major byproduct and the largest waste stream in petroleum production. Handling this water is a major issue in the oil industry. Gas flotation has proven to be an effective topside separation technology, and it is currently pursued for subsea produced water treatment. The combined effect of pressure and temperature on gas flotation has not been thoroughly investigated. In this study, we used a gas flotation rig to study the oil removal efficiency at elevated pressures and temperatures. Gas flotation experiments were performed up to 80 bar and 80 °C determining the oil removal at three different retention times. Gravity separation experiments at ambient temperature and elevated pressure conditions were used as a reference. The best oil removal was found at 80 °C in combination with high pressure. The temperature had the most significant impact on enhancing the separation, due to improved oil drop−gas bubble, gas bubble−gas bubble, and oil drop−oil drop coalescence due to the increased film thinning rates caused by lowered viscosity of the water, all leading to enhanced creaming. The pressure effect was attributed to more and smaller bubbles with increased pressures at a given temperature, increasing the available area for drop-bubble attachments. Finally, a first-order kinetic model described the gas flotation well.

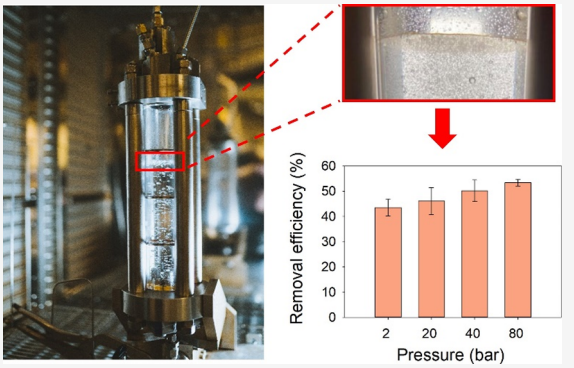


## 1. INTRODUCTION

One of the main environmental concerns related to oil production and processing is the disposal of produced water (PW), the largest waste stream generated in petroleum industry.[1,2] PW is extracted together with the hydrocarbons, and typically, it contains a complex mixture of dispersed and dissolved components which are environmentally harmful.[3,4] Worldwide, 3−5 barrels of produced water for each barrel of oil are generated,[5] resulting in ca. 250 million PW barrels per day.[6] PW is either discharged to the sea or re-injected. In both cases, the water must be treated to required qualities.

At the Norwegian Continental Shelf (NCS), according to the OSPAR regulations, (Oslo-Paris Convention for the Protection of the Marine Environment of the North-East Atlantic), the monthly-average discharge limit for oil is set to 30 mg/L. Recently, the European Commission aims to minimize the discharge to <15 mg/L for the existing installation and zero discharge on new facilities.[7] With these new and stricter regulations, re-injection is receiving more attention as an environmentally friendly and potentially cost-effective option.[8]

The traditional way of handling PW offshore involves transport of the water to a topside platform, where it undergoes different separation treatments before re-injection or discharge to the sea. Gas flotation (GF) is an efficient and common PW treatment, often preceded by gravity separators and hydrocyclone units.

There are two main flotation methods: induced gas flotation (IGF) and dissolved gas flotation (DGF). IGF and DGF differ in the way of generating bubbles and result in different bubble sizes, mixing conditions, hydraulic loading rate, and retention times. During the last decades, compact flotation units (CFUs), merging the advantages of both IGF and DGF, have been installed offshore, since the combination of the two methods leads to better oil removal efficiencies.[9] Recently, field tests were conducted with OiW concentrations ranging from 200 to 2000 ppm, reaching outlet oil concentrations between 2.5 and 21 ppm.[10]

One of the GF mechanisms relies on the attachment of the dispersed gas bubbles to the dispersed oil droplets. The new aggregates are both bigger and considerably less dense, so they

**Received:** December 1, 2022
**Revised:** March 3, 2023
**Published:** March 14, 2023

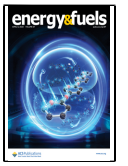







https://doi.org/10.1021/acs.energyfuels.2c04058
*Energy Fuels* 2023, 37, 5644−5651

can rise much faster to the surface.[11] Flotation is more efficient when the oil droplets spread over the gas bubbles' surface since detachment by the shear forces is minimized. It was reported that the rate governing step of flotation is the drainage of the water film between oil droplets and gas bubbles when they approach each other.[12]

Recently, more attention has been given to subsea PW treatment, together with the overall subsea production and processing systems, and it is expected to grow even further in the near future.[13] The reason being that the oil reserves in easily accessible locations are slowly running out, and the conventional topside production and processing become more difficult and cost-prohibitive.[3,14] Shifting the fluid processing to subsea is believed to lead to higher production and reduced costs,[15] in addition to advantages like reduced environmental impact and improved personnel safety[13,16]. The remote locations pose several challenges in terms of reliability of the subsea equipment and the need for minimization of subsea interventions.[17] Subsea produced water treatment can also avoid $CO_2$ emissions since less energy is required for pumping of fluids to the topside level.[18] Currently, subsea oil−water separation installations are the Troll-Pilot and Tordis gravity separators at the Norwegian Continental Shelf, and the hydrocyclones,[19] installed at the Brazilian Marlim field.[20] It was reported that the gravity separators give an oil outlet concentration of 500−600 mg/L, which is too high for the PW to be disposed to the sea.[21] Moreover, turndown, fouling, and separation of oil droplets smaller than 10 microns become challenging when using hydrocyclones.[18] Given this, a secondary treatment method might be needed to reach either discharge or re-injection quality of the water.

Gas flotation is considered a good candidate for subsea PW water treatment technologies. Different factors and conditions that can influence its efficiency at ambient conditions (e.g., salinity, surfactants, pH etc.) have been reported.[9,22−25]

Younker and Walsh[22] investigated dissolved air flotation (DAF) at the bench scale for the removal of dispersed and dissolved oils from synthetic and offshore produced water. Their results showed high removal of dispersed oil, especially when the flotation was combined with coagulation treatment. Painmanakul et al.[23] used induced air flotation in a column with rigid and flexible orifice gas diffusers to study the treatment of oily wastewater. The oil removal was related to the pH and gas flow rate and improved when the flotation was combined with chemical aids/coagulation treatment.

Chakibi et al.[24] conducted a study to test the effect of salinity of produced water, highlighting the importance of the electrostatic repulsion between oil droplets and gas bubbles. They demonstrated that increasing the salinity improved the attachment between gas bubbles and oil droplets, as the electrostatic repulsions between bubbles and droplets were weakened, causing faster drainage of the liquid film.

Asdahl et al.[25] examined the applicability and effectiveness of using CFU technology in heavy crude oil PW treatment. They observed that for a given oil, high oil removal efficiency was favored by larger oil droplets. For different API crude oils with the same droplet size, a moderate reduction in the efficiencies was observed for heavy crude oils.

Eftekhardadkhah et al.[9] tested the oil removal from PW both on a laboratory and pilot scale. Laboratory scale experiments with three different crude oils showed better oil removal efficiencies when decreasing the coalescence time. In the pilot scale studies, both DGF and IGF were tested, and the highest removal was obtained when they were combined.

A few studies on the effect of temperature on flotation have also been carried out.[26−28] Strickland[26] investigated the temperature effect on oil recovery using gas flotation, obtaining higher efficiencies when working at 60 °C than at ambient conditions. Mastouri et al.[27] investigated the effect of temperature on the performance of IGF systems for the removal of oil from PW in different ranges of total dissolved solids (TDS). They obtained increased oil removal efficiencies when the temperature was raised from 20 to 80 °C at high TDS. Then, oil removal diminished up to 100 °C.

Qi et al.[28] treated alkali/surfactant/polymer wastewater using loop-flow flotation in a temperature range from 10 to 40 °C. They observed improved removal rate with increased temperature, reaching a recovery of ca. 93% at the highest temperature. This was attributed to accelerated coalescence of the oil droplets due to decreased elasticity and viscosity of the interfacial layer, while drop−bubble attachments were not considered.

To the best of our knowledge, only Zhao et al.[18] reported the combined effects of high temperature and high pressure on oil removal. Using an experimental design, they identified increased pressure and reduced water flow rates as the two variables with the largest effect on the oil removal efficiency.

In this work, a method for performing laboratory-scale high-pressure and high-temperature gas flotation experiments was developed. The combined effects of temperature and pressure on the oil removal from synthetic produced water were studied by systematic combinations of pressure and temperature conditions up to 80 bar and 80 °C, respectively. In addition, gravity separation experiments at ambient temperature and various pressure conditions were performed for reference. The results were implemented in a first-order kinetic model.

## 2. METHODS

**2.1. Crude Oil.** The investigated crude oil was produced at the Norwegian Continental Shelf (NCS). It was denoted as crude oil G, for consistency with previous reports from our group.[29,30] A summary of the physicochemical properties of the oil is given in Table 1, while the full characteristics and the description of experimental methods were reported elsewhere.[29,30]

**Table 1. Physicochemical Properties of Crude Oil G[29]**

| | |
|---|---|
| density at 20 °C (g/cm$^3$) | 0.85 |
| viscosity at 20 °C (mPa*s) | 12.4 |
| TAN (mg/g) | 0.2 |
| TBN (mg/g) | 0.6 |
| saturates (wt %) | 83.4 |
| aromatics (wt %) | 14.0 |
| resins (wt %) | 2.4 |
| asphaltenes (wt %) | 0.2 |
| API (°) | 34.5 |

**2.2. Preparation of Oil-in-Water Emulsion (OiW).** OiW emulsions (250 mL) were prepared by dispersing the crude oil in 3.5 wt % sodium chloride (p.a., Merck Millipore, USA) solutions. This salt concentration was chosen since it is similar to the seawater salinity and the PW salinity at the NCS,[31] while the composition was limited to sodium chloride to avoid effects of multivalent ions. For the experiments performed at 50 and 80 °C, the samples were pre-heated before emulsification to avoid separation due to heating in the flotation column. The samples were emulsified using an Ultra-Turrax mixer for 5 min at 15,000 rpm. The initial oil concentration was set to


https://doi.org/10.1021/acs.energyfuels.2c04058
Energy Fuels 2023, 37, 5644−5651

ca. 220 ppm, resembling a worst-case scenario on a typical NCS installation and to get stronger impact on parameters being varied during testing.

The size distributions of the emulsions were determined using a Malvern Mastersizer 3000 − Particle analyzer. Four parallels were measured at each temperature and the averaged droplets size distributions are presented in Figure 1. The size distribution for the

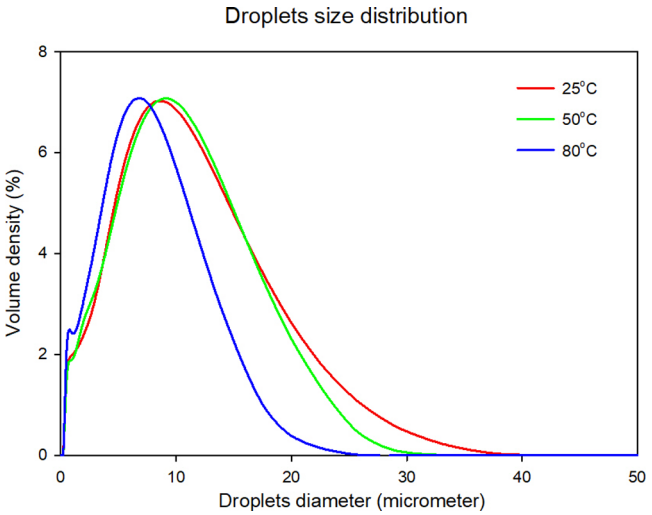


**Figure 1.** Oil droplet size distribution at different temperature values. Each distribution is the average of four different measurements.

emulsions mixed at 80 °C is slightly smaller than that for those mixed at 25 and 50 °C. This can be due to the lower viscosity of the oil at higher temperatures, which makes the oil easier to disperse. To evaluate if this difference in the drop size distributions would affect the separation significantly, the Stokes law (eq 1) was used to calculate the creaming rates:

$$v = \frac{2}{9}\frac{R^2(\rho_o - \rho_w)}{\mu}g \quad (1)$$

where "$v$" is the velocity of droplets, $\rho_o$ and $\rho_w$ are the density of the oil and water phase, respectively, $\mu$ is the viscosity of the water phase, "$g$" is the acceleration due to gravity, and $R$ is the radius of the oil droplets.

The creaming rates were calculated considering the Dv10, Dv50, and Dv90 values for each temperature. Table 2 lists the drop sizes, creaming rates, and corresponding rising distances after 3 and 20 min. The rising distances were within the same order of magnitude for the

**Table 2. Dv10,50,90 Diameters and Creaming Rates at Different Temperatures**[a]

| temperature (°C) | Dv($x$) | droplets diameter ($\mu$m) | creaming rate ($\mu$m/s) | settling distance (mm) after 3 min | settling distance (mm) after 20 min |
|---|---|---|---|---|---|
| 25 | Dv10 | 0.8 | 0.1 | 0.0 | 0.1 |
| | Dv50 | 5.7 | 3.0 | 0.5 | 3.6 |
| | Dv90 | 15.5 | 22.3 | 4.0 | 26.8 |
| 50 | Dv10 | 0.8 | 0.1 | 0.0 | 0.1 |
| | Dv50 | 5.8 | 5.4 | 0.9 | 6.5 |
| | Dv90 | 14.8 | 34.6 | 6.2 | 41.5 |
| 80 | Dv10 | 0.7 | 0.1 | 0.0 | 0.1 |
| | Dv50 | 4.21 | 4.5 | 0.8 | 5.4 |
| | Dv90 | 10.6 | 28.2 | 5.1 | 33.8 |

[a]Settling distance after 3 and 20 min was also calculated

various temperatures, and it was assumed that the emulsions were comparable.

**2.3. High-Pressure and High-Temperature Gas Flotation Setup.** The gas flotation experiments were carried out using a high-pressure and high-temperature gas flotation rig designed and built in-house. The standard setup of the rig is illustrated in Figure 2. A 360

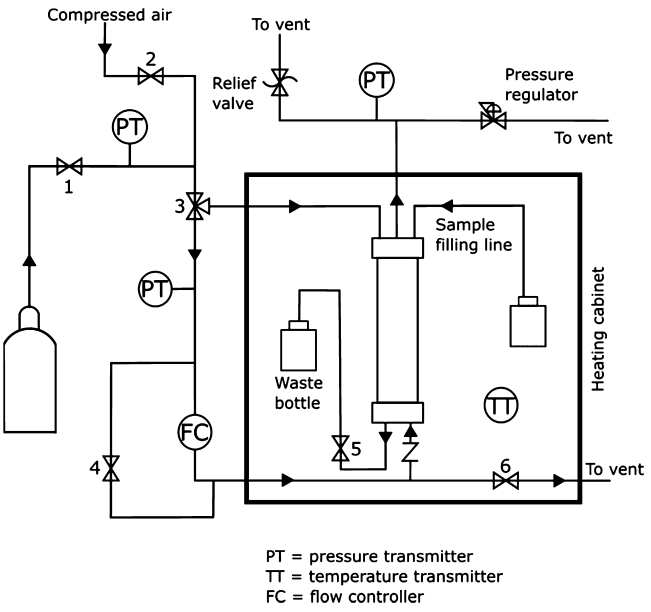


**Figure 2.** Schematic representation of the flotation rig.

cm$^3$ flotation column, made of sapphire glass, was placed inside a heating cabinet (Memmert UN750). The gas was dispersed from the bottom of the column into the emulsion with stainless-steel micro-spargers provided by GKN Sinter Metals Filters GmbH (SIKA-R, filter efficiency in micron: 5, porosity: 5−31%). All the flotation experiments were performed with nitrogen, and the flow of gas was controlled with a gas flow controller (EL-Flow Prestige FG-211CV, Bronkhorst High-Tech B.V., The Netherlands).

Three stainless-steel pressure transmitters (DMP 333 - BD SENSORS, range 0−100 bar/4-20 mA) were installed on three different lines on the rig ("PT" in Figure 2), while a temperature sensor ("TT" in Figure 2) (Omega, operating temperature −50 to 260 °C, resistance at 0 °C 100 Ω) was placed inside the heating cabinet. The pressure and temperature sensors were connected to a C Series current input module (NI-9203, National Instrument) and a C Series temperature input module (NI-9217, National Instrument), respectively. The analog signal from the C Series Modules was converted into digital through a Compact DAQ USB Chassis (NI-9171, National Instrument). The temperature and pressure values were monitored through a custom-written script in the LabVIEW software.

*2.3.1. Gas Flow.* Due to increasing solubility of nitrogen,[32] the amount of gas bubbles decreased considerably at constant gas flows and increasing pressures (Figure S1). To ensure comparable volume fractions of gas bubbles at all the working conditions, the gas flow had to be increased when raising the pressure, as summarized in Table 3. These gas flow rates were determined by measuring the intensity (pixel) of light passing through the column when 3.5 wt % NaCl brine was subjected to different combinations of pressure and gas flow rates. Five different pressure values were investigated at six different gas flows (Table S1 in the Supporting Information). For each combination of gas flow and pressure value, 10 images were taken with a high-speed camera (Canon Eos 90D, AX100, Photron, Japan). The mean intensity of the pictures was calculated with ImageJ software, using a section of the entire column. (Figure 3). For every condition, the experiments were repeated three times to ensure reproducibility. The intensities versus gas flows are shown in the


https://doi.org/10.1021/acs.energyfuels.2c04058
Energy Fuels 2023, 37, 5644−5651

**Table 3. Overview of the Gravity Separation and Gas Flotation Experimental Conditions**[a]

| pressure (bar) | gas flow (mL/min) | temperature (°C) | flotation/residence time (min) |
|---|---|---|---|
| 2 | 50 | 25, 50, 80 | 3, 10, 20 |
| 20 | 300 | 25, 50, 80 | 3, 10, 20 |
| 40 | 600 | 25, 50, 80 | 3, 10, 20 |
| 80 | 1200 | 25, 50, 80 | 3, 10, 20 |

[a]Gas flows are given in standard conditions.

Supporting Information (Figure S2 and Table S2). The gas flows which gave the closest mean intensity of the image sets, at different pressure conditions, were chosen. Images of the gas bubbles at the selected gas flows are shown in Figure 3.

*2.3.2. Experimental Procedure.* Flotation experiments were performed at different pressures (2, 20, 40, and 80 bar) and temperatures (25, 50, and 80 °C). In addition, gravity separation (i.e., experiments without introducing gas bubbles) was carried out as the baseline for the flotation experiments. These experiments were carried out at the same four pressures at 25 °C. The lower temperature was set to have a reference point to other gas flotation studies, typically performed at ambient conditions, while the higher temperature approached the limitations of the setup. The pressure values were chosen to have a broad span of pressures since this parameter is little studied in the literature.

Three parallels of each parameter combination were run to ensure reproducibility. The error bars in Figures 4 and 5 represent the standard deviations calculated from the different parallels. The procedure for performing the experiments is explained in the following.

First, the inlet pressure was set to a value that was approximately 20% above the test pressure at the gas bottle regulator, with Valve 1 closed. Next, the emulsion was introduced to the flotation column through a removable funnel. The cell was then tightly closed, and the pressure regulator was set to the test value. The volume above the sample was pressurized by opening Valve 1 and directing the gas to the top of the sample through Valve 3. It took ca. 1.5 min from the end of the emulsification process until a stable pressure was reached. This was the starting point for the gravity separation experiments. For the gas flotation experiments, Valve 3 was switched to redirect the gas to the bottom of the cell through a gas flow controller (FC), which was pre-set to the pressure and flow values of the experiment.

To facilitate the flow of gas through the spargers, the pressure on the inlet side of the FC had to be 20% higher than the outlet pressure, set at the pressure regulator before. For this reason, the pressure set at the gas bottle was always higher than the test pressure. Since the solubility of nitrogen increased with pressure, the time needed for the bubbles to appear varied between the different tested conditions. These are summarized in Table 4. The appearance of the bubbles marked the beginning of the flotation experiments.

Oil removal was determined after 3, 10, and 20 min (in separate experiments). Approximately, 150 mL of sample was collected under pressure through a line connected to the bottom of the cell by carefully opening Valve 5. After sampling, the pressure was released from the system by reducing the set pressure on the pressure regulator and opening Valve 6. After every experiment, the flotation cell was cleaned with xylene, isopropanol, and water. Compressed air was flown through the top (Valve 3 switched to the top of the cell) and the bottom (Valve 3 switched to the bottom of the cell and with open bypass of the FC Valve 4) of the cell, first to remove the solvents and later to dry the cell. Approximately, 100 mL of the collected water samples was mixed with dichloromethane (DCM). The exact weights of the samples were recorded to calculate the oil concentrations. A glass separation funnel was used to separate the organic phase, containing the extracted crude oil components and the water. The organic solutions were analyzed using ultraviolet spectroscopy (Agilent Cary 3500 UV−vis double beam spectrophotometer). The absorbance at 260 nm was used to determine the amount of crude oil extracted into the organic phase, using a pre-made calibration curve (10−230 ppm) of the crude oil dissolved in DCM. Finally, the oil removal efficiency was calculated according to the following equation (eq 2):

$$\text{Oil removal efficiency} = \frac{C_i - C_f}{C_i} \tag{2}$$

where $C_i$ is the oil concentration of the initial emulsion and $C_f$ is the crude oil concentration after 3, 10, and 20 min of flotation (or gravity separation).

**2.4. Flotation Kinetics.** The kinetics of bubble-oil droplets collision and coalescence can be defined by the following differential equation (eq 3):[33]

$$\frac{dC}{dt} = -kC^n \tag{3}$$

where $C$ is the concentration of oil droplets, "$k$" is the flotation rate constant, "$n$" is the kinetic order, and "$t$" is the flotation time. According to Nguyen and Schulze,[34] flotation processes are generally between first and second order kinetics, while it can be simplified to first-order kinetics for very dilute dispersions and to second-order kinetics for more concentrated ones. Since the emulsions in this study were diluted, it was assumed that the rate of bubbles−droplets collision was of first-order kinetics,[35] and eq 3 can be written (eq 4) as follows:

$$\frac{dC}{dt} = -kC \tag{4}$$

The integration of eq 4 leads to eq 5:

$$C(t) = C_i e^{(-kt)} \tag{5}$$

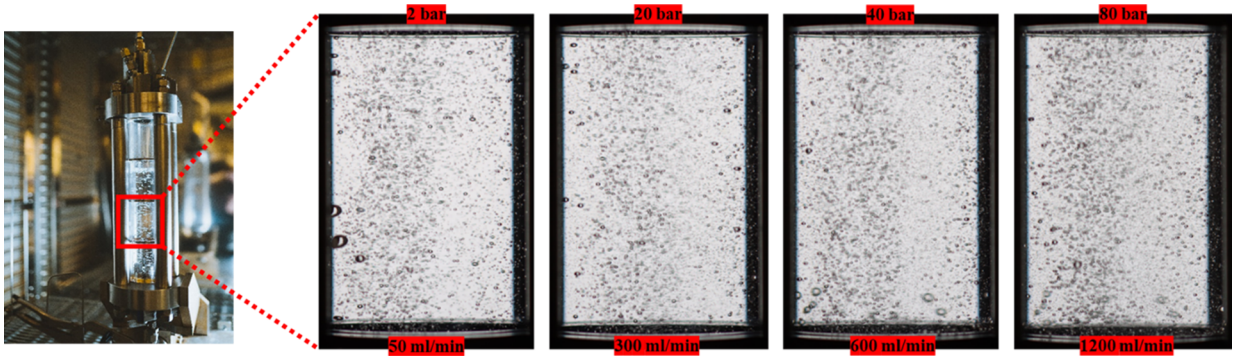


**Figure 3.** Images of the volume fraction of bubbles at the pressures and the flow rates used here.



https://doi.org/10.1021/acs.energyfuels.2c04058
Energy Fuels 2023, 37, 5644−5651

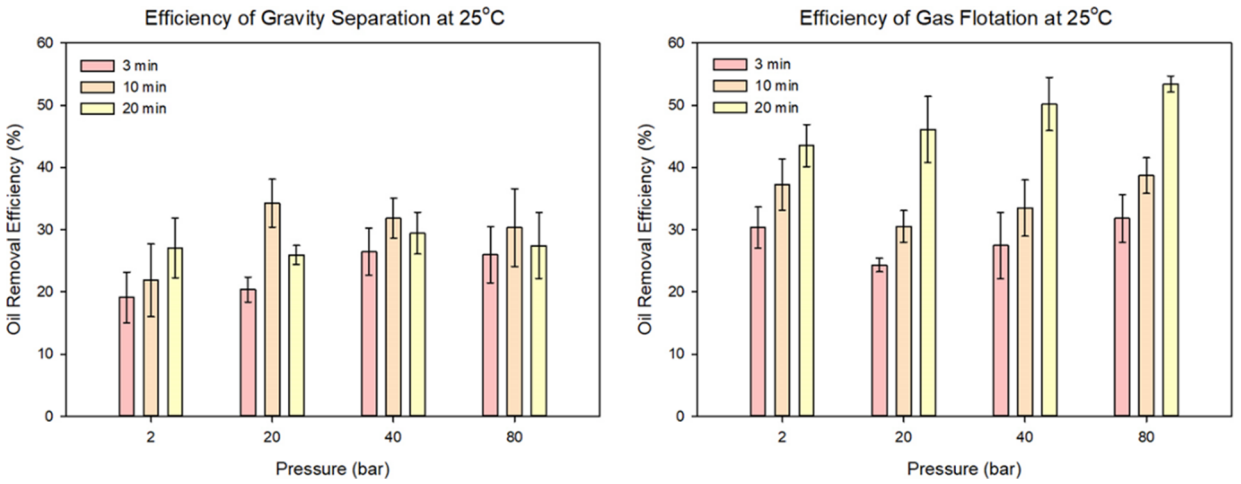


**Figure 4.** Oil removal efficiencies after gravity separation (left) and gas flotation (right) at 25 °C. Experiments were performed at four pressure values and three residence times.

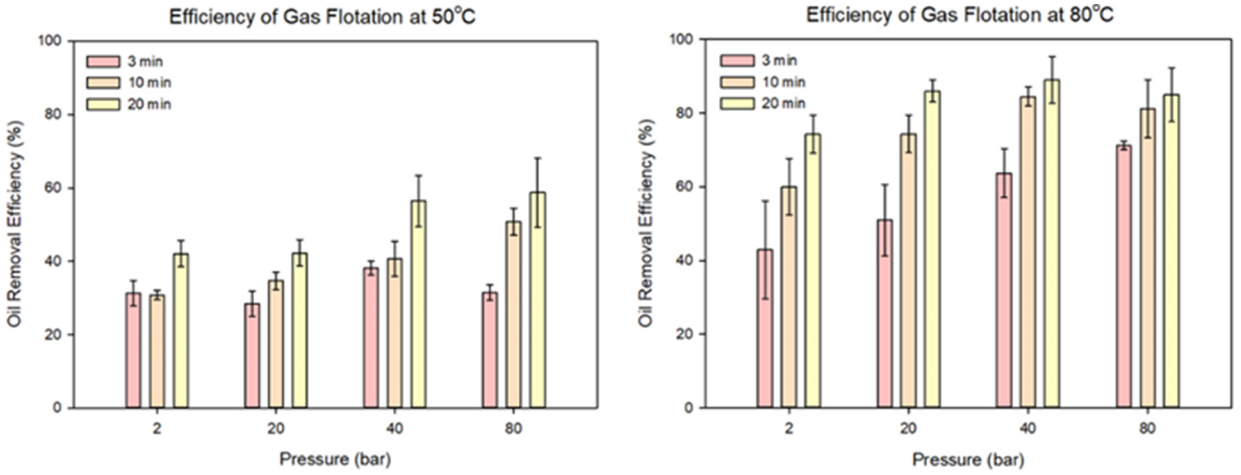


**Figure 5.** Oil removal efficiency after gas flotation at 50 °C (left) and 80 °C (right). The experiments were performed at four different pressures and three residence times.

**Table 4. Time Needed for the Bubbles To Appear in the Flotation Column for Different Experimental Pressures**

| pressure (bar) | time (min) |
|---|---|
| 2 | 0.34 |
| 20 | 0.59 |
| 40 | 1.01 |
| 80 | 1.51 |

The values of the rate constants were determined from the slope of plotting the natural logarithm of the oil concentration ($\ln C_t$) against the flotation time ($t$).

## 3. RESULTS AND DISCUSSION

**3.1. Gravity Separation and Gas Flotation at Ambient Temperature and Elevated Pressures.** The oil removal efficiencies after gravity separation and gas flotation at 25 °C are presented in Figure 4.

Overall, the gas flotation improved the oil removal efficiency compared to gravity separation at all pressures tested. The highest oil removal was found to be 53% at 80 bar after 20 min. Unlike gravity separation, gas flotation improved oil removal over time. Furthermore, a 10% increase in the separation efficiency was seen when the pressure was increased from 2 to 80 bar in the flotation experiments with 20 min residence time.

Without introducing gas bubbles, the separation was mainly due to coalescence between the oil droplets and creaming. Considering the estimated creaming rates (Table 2), the biggest oil droplets (Dv90) would only raise 2.7 cm after 20 min, while the height of the sample inside the column was 21 cm (Figure S3, Supporting Information). This means that coalescence of oil droplets must have played a significant role to reach the observed oil removal. The flotation results were considered in view of the attachment between oil droplets and gas bubbles, leading to stable aggregates that can withstand the shear forces during flotation. Prior to such attachment, a thin water film was created between the approaching oil droplets and gas bubbles. Eftekhardadkhah et al. demonstrated that quick drainage of this film improved the oil removal efficiency.[9] The effect of temperature and pressure on these experiments are discussed in the following.

**3.2. Gas Flotation at Higher Temperatures and Elevated Pressures.** Oil removal efficiencies after gas flotation experiments performed at 50 and 80 °C are presented in Figure 5.



https://doi.org/10.1021/acs.energyfuels.2c04058
Energy Fuels 2023, 37, 5644−5651

The removal efficiency increased considerably at all retention times and pressures when the temperature was increased from 50 to 80 °C. Oil removal was already more than 40% after 3 min flotation at 2 bar at 80 °C, while the highest removals were 85 and 89% with 20 min retention time at 80 and 40 bar, respectively. Furthermore, oil removal increased with longer duration of the flotation.

When comparing the gas flotation at 25 °C (Figure 4) and 50 °C (Figure 5), however, there was little improvement in oil removal. At lower pressures, there was even a slight reduction in the oil removal when increasing the temperature. Nevertheless, the removal efficiency increased with pressure for all the residence time at 80 °C.

The impact of temperature and pressure on the first-order rate constants is shown in Figure 6. The values can be found in

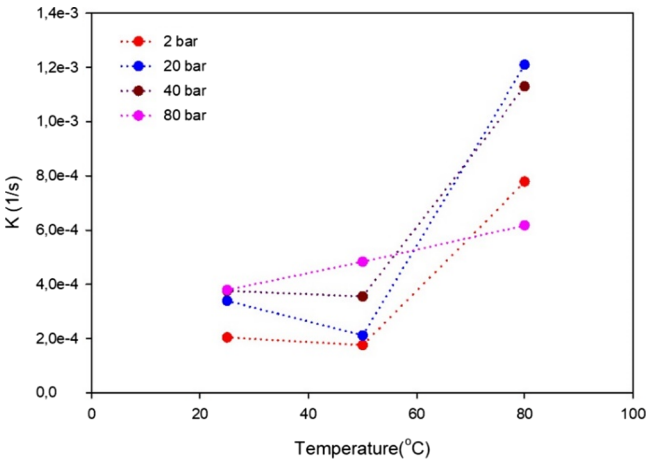


**Figure 6.** Effect of temperature and pressure on the rate constant values.

Table S3 in the Supporting Information. The trends were similar as described for the oil removal, with relatively similar rate constants at 20 and 50 °C and a marked increase at 80 °C. Shahrezaei et al.[36] also observed an increase of the rate constant with temperature in their wastewater treatment studies. The highest values of the rate constant were found at 80 °C, while a pressure trend, observed at lower temperature, was not seen at this temperature.

*3.2.1. Effect of Temperature.* Raising the temperature decreased the viscosity and density of all the phases. The viscosity of water has been reported to decrease almost by 60% when the temperature increases from 20 to 70°C.[37] This will lead to higher rising velocities of bubbles and droplets in accordance with the Stokes law. The increased temperature will also increase the thermal energy in the emulsions, leading to enhanced collision frequencies between the dispersed components. The reduced viscosity of the water will also lead to enhanced film thinning rates between bubbles and droplets, resulting in faster drop bubble attachments as well as drop-drop and bubble-bubble coalescence, and ultimately better separation. Furthermore, Jones et al. reported the existence of a kinetic barrier to coalescence at a temperature as high as 65 °C, due to the slow relaxation process in interfacial films. Such barriers could explain the small change in removal efficiency when going from 25 to 50 °C.[38]

*3.2.2. Effect of Pressure.* Increasing pressure resulted in increased density of the gas phase, which gave smaller bubble sizes and narrower bubble size distributions (Figure S7 and measurement procedures in the Supporting Information). Similar trends were observed also by other research groups[39−41] This also implied that more bubbles were present at higher pressures at a given temperature, for the volume fraction of bubbles to be similar at all the pressures. Bubble breakage could also be a reason for smaller bubble sizes. This could be due to a larger inertia of the gas at higher densities, as reported by others.[39] Another effect of increasing pressure was the increased amounts of dissolved gas in the oil and aqueous phases, reducing the densities of both phases, but more significantly for oil than for water.[18,39] Nevertheless, the dissolved gas in the aqueous phase would decrease the surface tension of the bubbles, which could also facilitate breakup of the bubbles.[18,42] Independent of the reason for more, smaller bubbles with increased pressure at a given temperature, a larger total area of bubbles was available for interaction with oil, increasing the probability of drop−bubble attachments. Moreover, it was shown that small gas bubbles have shorter coalescence times.[43]

## 4. CONCLUSIONS

A gas flotation setup and a method to study the oil removal efficiency at high pressures and temperatures were developed.

Systematic gravity separation and gas flotation experiments were performed at different pressures, temperatures, and separation times to study the oil removal efficiency. As expected, gas flotation improved the separation process compared to gravity separation, which was explained by the drop-gas bubble attachment mechanism, in addition to drop-drop and bubble-bubble coalescence. Moreover, gas flotation improved oil removal over the investigated time.

Gas flotation was most efficient at the highest temperature tested (80 °C) in combination with high pressure. This demonstrated an interplay between temperature and pressure in enhancing the separation. Increasing the temperature had the most dominant effect, due to improved creaming and (drop−bubble, bubble−bubble, and drop−drop) coalescence rates when the viscosity of the water decreased. However, a temperature threshold had to be overcome before the separation improved at all conditions. Increasing the pressure improved the oil removal by increasing the bubble area available for oil attachments.

## ■ ASSOCIATED CONTENT

### Supporting Information

The Supporting Information is available free of charge at https://pubs.acs.org/doi/10.1021/acs.energyfuels.2c04058.

Images of gas bubbles inside the flotation column at 2, 20, 40 and 80 bar when a gas flow of 50 mL/min is applied in a 3.5 wt % NaCl brine; table with all the tested gas flows at 2, 20, 40, 60, and 80 bar; graph representing the trend of the intensity of light (pixels) with the tested gas flows; table with the selected gas flows and their average light intensities for each pressure condition; kinetic parameters for all the pressure and temperature conditions tested during the gas flotation experiments; sample height inside the flotation column; image representing the four different mechanisms for gas bubble capture of oil droplets suspended in water; microfluidic snapshot showing the different stages of oil droplet and gas bubble interaction and attachment; procedure describing the gas bubble distribution study



https://doi.org/10.1021/acs.energyfuels.2c04058
Energy Fuels 2023, 37, 5644−5651

with an image representing the bubbles in NaCl brine captured by a camera; and graph showing the gas bubble distributions at the four pressure conditions tested: 1, 10, 30, and 50 bar (PDF)

## AUTHOR INFORMATION


### Corresponding Author

**Gisle Øye** − *Ugelstad Laboratory, Department of Chemical Engineering, Norwegian University of Science and Technology (NTNU), N-7491 Trondheim, Norway;* orcid.org/0000-0002-6391-3750; Email: gisle.oye@ntnu.no

### Authors

**Martina Piccioli** − *Ugelstad Laboratory, Department of Chemical Engineering, Norwegian University of Science and Technology (NTNU), N-7491 Trondheim, Norway;* orcid.org/0000-0001-9482-4745

**Robert André Gjelsten Larsen** − *Ugelstad Laboratory, Department of Chemical Engineering, Norwegian University of Science and Technology (NTNU), N-7491 Trondheim, Norway*

**Marcin Dudek** − *Ugelstad Laboratory, Department of Chemical Engineering, Norwegian University of Science and Technology (NTNU), N-7491 Trondheim, Norway;* orcid.org/0000-0001-6444-7109

**Svein Viggo Aanesen** − *Equinor Research Centre, N-3905 Porsgrunn, Norway*

Complete contact information is available at: https://pubs.acs.org/10.1021/acs.energyfuels.2c04058


### Notes

The authors declare no competing financial interest.

## ACKNOWLEDGMENTS

This work was carried out as a part of SUBPRO, a Research based Innovation Centre within Subsea Production and Processing. The authors gratefully acknowledge the financial support from SUBPRO, which is financed by the Research Council of Norway, major industry partners, and NTNU. We additionally thank Yasaman Hajizadeh for performing some of the gas flotation experiments.

## REFERENCES


(1) Liu, Y.; Lu, H.; Li, Y.; Xu, H.; Pan, Z.; Dai, P.; Wang, H.; Yang, Q. A review of treatment technologies for produced water in offshore oil and gas fields. *Sci. Total Environ.* **2021**, *775*, No. 145485.

(2) Al-Ghouti, M. A.; Al-Kaabi, M. A.; Ashfaq, M. Y.; Da'na, D. A. Produced water characteristics, treatment and reuse: A review. *J. Water Process Eng.* **2019**, *28*, 222−239.

(3) Piccioli, M.; Aanesen, S. V.; Zhao, H.; Dudek, M.; Øye, G. Gas Flotation of Petroleum Produced Water: A Review on Status, Fundamental Aspects, and Perspectives. *Energy Fuels* **2020**, *34*, 15579−15592.

(4) Ghafoori, S.; Omar, M.; Koutahzadeh, N.; Zendehboudi, S.; Malhas, R.; Mohamed, M.; Al-Zubaidi, S.; Redha, K.; Baraki, F.; Mehrvar, M. New Advancements, Challenges, and Future Needs on Treatment of Oilfield Produced Water: A State-of-the-Art Review. *Sep. Purif. Technol.* **2022**, *289*, No. 120652.

(5) Fakhru'l-Razi, A.; Pendashteh, A.; Abdullah, L. C.; Biak, D. R.; Madaeni, S. S.; Abidin, Z. Z. Review of technologies for oil and gas produced water treatment. *J. Hazard. Mater.* **2009**, *170*, 530−551.

(6) Amakiri, K. T.; Canon, A. R.; Molinari, M.; Angelis-Dimakis, A. Review of oilfield produced water treatment technologies. *Chemosphere* **2022**, *298*, No. 134064.

(7) Commission, E. In *Best Available Techniques Guidance Document on upstream hydrocarbon exploration and production*; Limited, W. E., Infrastructure Solutions, U. K., Eds.; Publications Office of the European Union: Luxembourg, 2019.

(8) Azizov, I.; Dudek, M.; Øye, G. Studying droplet retention in porous media by novel microfluidic methods. *Chem. Eng. Sci.* **2022**, *248*, No. 117152.

(9) Eftekhardadkhah, M.; Aanesen, S. V.; Rabe, K.; Øye, G. Oil Removal from Produced Water during Laboratory- and Pilot-Scale Gas Flotation: The Influence of Interfacial Adsorption and Induction Times. *Energy Fuels* **2015**, *29*, 7734−7740.

(10) Asdahl, S.; Jansen van Rensburg, J.; Waag, M. E.; Glenna Nilssen, R. Cost-Efficient De-Bottlenecking of Produced Water Treatment Systems through the Application of a Single Technology, Eliminating the Need for Hydrocyclones and Degassing Drums. In *Abu Dhabi International Petroleum Exhibition & Conference*, 2021.

(11) Moosai, R.; Dawe, R. A. Oily Wastewater Cleanup by Gas Flotation. *West Indian J. Eng.* **2002**, *25*, 25.

(12) Moosai, R.; Dawe, R. A. Gas attachment of oil droplets for gas flotation for oily wastewater cleanup. *Sep. Purif. Technol.* **2003**, *33*, 303−314.

(13) Bhardwaj, U.; Teixeira, A. P.; Guedes Soares, C. Bayesian framework for reliability prediction of subsea processing systems accounting for influencing factors uncertainty. *Reliab. Eng. Syst. Saf.* **2022**, *218*, No. 108143.

(14) Bai, Y.; Bai, Q. *Subsea engineering handbook*; Gulf Professional Publishing, 2018.

(15) da Silva, F. S.; Monteiro, A. S.; de Oliveira, D. A.; Capela Moraes, C. A.; Marins, P. M. In *Subsea Versus Topside Processing − Conventional and New Technologies*; OTC Brasil: Rio de Janeiro, Brazil, 2013.

(16) Devegowda, D.; Scott, S. L. An Assessment of Subsea Production Systems. In *SPE Annual Technical Conference and Exhibition*, 2003; SPE-84045-MS, Vol. All Days.

(17) Fanailoo, P.; Andreassen, G. Improving Reliability and Reducing Intervention Costs of Ultradeep Subsea Technology at the Design Stage. In *Offshore Technology Conference*, 2008.

(18) Zhao, H.; Berg, J. K.; Stinessen, K. O.; Solumsmoen, G. B.; Kolbu, J.; Johnsen, K. H.; Knudsen, B. L.; Gudbrandsen, K. A.; Rondon, M.; Berthelot, A.; et al. High Pressure Testing of a Pilot Subsea Compact Flotation Unit. In *Offshore Technology Conference*; Houston, Texas, USA, 2020.

(19) Skjefstad, H. S.; Stanko, M. Subsea water separation: a state of the art review, future technologies and the development of a compact separator test facility. In *18th International Conference on Multiphase Production Technology*; Cannes, France, 2017.

(20) Mishiga Vallabhan, K. G.; Holden, C.; Skogestad, S. A First-Principles Approach for Control-Oriented Modeling of De-oiling Hydrocyclones. *Ind. Eng. Chem. Res.* **2020**, *59*, 18937−18950.

(21) Horn, T.; Bakke, W.; Eriksen, G. Experience in operating World's first Subsea Separation and Water Injection Station at Troll Oil Field in the North Sea. In *Offshore Technology Conference*, Houston, Texas, 2003.

(22) Younker, J. M.; Walsh, M. E. Impact of salinity on coagulation and dissolved air flotation treatment for oil and gas produced water. *Water Qual. Res. J. Can.* **2014**, *49*, 135−143.

(23) Painmanakul, P.; Sastaravet, P.; Lersjintanakarn, S.; Khaodhiar, S. Effect of bubble hydrodynamic and chemical dosage on treatment of oily wastewater by Induced Air Flotation (IAF) process. *Chem. Eng. Res. Des.* **2010**, *88*, 693−702.

(24) Chakibi, H.; Hénaut, I.; Salonen, A.; Langevin, D.; Argillier, J. F. Role of Bubble−Drop Interactions and Salt Addition in Flotation Performance. *Energy Fuels* **2018**, *32*, 4049−4056.

(25) Asdahl, S.; Maelum, M.; Rabe, K. Heavy Oil-Produced Water Polishing with Compact Flotation Technology. In *SPE Heavy Oil Conference and Exhibition*, Kuwait City, Kuwait; 2016.

(26) Strickland, W. T., Jr. Laboratory Results of Cleaning Produced Water by Gas Flotation. *Soc. Pet. Eng. J.* **1980**, *20*, 175−190.

(27) Mastouri, R.; Borghei, S. M.; Nadim, F.; Roayaei, E. The Effect of Temperature and Impeller Speed on Mechanically Induced Gas Flotation (IGF) Performance in Separation of Oil from Oilfield-Produced Water. *Pet. Sci. Technol.* **2010**, *28*, 1415−1426.
(28) Qi, W.-K.; Yu, Z.-C.; Liu, Y.-Y.; Li, Y.-Y. Removal of emulsion oil from oilfield ASP wastewater by internal circulation flotation and kinetic models. *Chem. Eng. Sci.* **2013**, *91*, 122−129.
(29) Dudek, M.; Chicault, J.; Øye, G. Microfluidic Investigation of Crude Oil Droplet Coalescence: Effect of Oil/Water Composition and Droplet Aging. *Energy Fuels* **2020**, *34*, 5110−5120.
(30) Dudek, M.; Ullaland, H. S.; Wehrle, A.; Øye, G. Microfluidic testing of flocculants for produced water treatment: Comparison with other methodologies. *Water Res.: X* **2020**, *9*, No. 100073.
(31) Ray, J. P.; Engelhardt, F. R. *Produced Water: Technological/Environmental Issues and Solutions*; Springer US, 1992.
(32) Sun, R.; Hu, W.; Duan, Z. Prediction of Nitrogen Solubility in Pure Water and Aqueous NaCl Solutions up to High Temperature, Pressure, and Ionic Strength. *J. Solution Chem.* **2001**, *30*, 561−573.
(33) Gharai, M.; Venugopal, R. Modeling of Flotation Process—An Overview of Different Approaches. *Miner. Process. Extr. Metall. Rev.* **2015**, *37*, 120−133.
(34) Nguyen, A. V.; Schulze, H. J. *Colloidal Science of Flotation*; CRC Press, 2003.
(35) Bu, X.; Xie, G.; Chen, Y.; Ni, C. The Order of Kinetic Models in Coal Fines Flotation. *Int. J. Coal Prep. Util.* **2017**, *37*, 113−123.
(36) Shahrezaei, F.; Mansouri, Y.; Zinatizadeh, A. A. L.; Akhbari, A. Process modeling and kinetic evaluation of petroleum refinery wastewater treatment in a photocatalytic reactor using TiO2 nanoparticles. *Powder Technol.* **2012**, *221*, 203−212.
(37) Bera, B.; Khazal, R.; Schroën, K. Coalescence dynamics in oil-in-water emulsions at elevated temperatures. *Sci. Rep.* **2021**, *11*, 10990.
(38) Jones, T. J.; Neustadter, E. L.; Whittingham, K. P. Water-In-Crude Oil Emulsion Stability And Emulsion Destabilization By Chemical Demulsifiers. *J. Can. Pet. Technol.* **1978**, *17*, PETSOC-78-02-08.
(39) Schäfer, R.; Merten, C.; Eigenberger, G. Bubble size distributions in a bubble column reactor under industrial conditions. *Exp. Therm. Fluid Sci.* **2002**, *26*, 595−604.
(40) Letzel, H. M.; Schouten, J. C.; Krishna, R.; van den Bleek, C. M. Gas holdup and mass transfer in bubble column reactors operated at elevated pressure. *Chem. Eng. Sci.* **1999**, *54*, 2237−2246.
(41) Luo, X.; Lee, D. J.; Lau, R.; Yang, G.; Fan, L.-S. Maximum stable bubble size and gas holdup in high-pressure slurry bubble columns. *AIChE J.* **1999**, *45*, 665.
(42) Lee, J. I.; Yim, B.-S.; Kim, J.-M. Effect of dissolved-gas concentration on bulk nanobubbles generation using ultrasonication. *Sci. Rep.* **2020**, *10*, 18816.
(43) Gu, G.; Xu, Z.; Nandakumar, K.; Masliyah, J. Effects of physical environment on induction time of air−bitumen attachment. *Int. J. Miner. Process.* **2003**, *69*, 235−250.





https://doi.org/10.1021/acs.energyfuels.2c04058
*Energy Fuels* 2023, 37, 5644−5651